chemengineering

MDPI

Supplementary Material:

Mitigation of Cr(VI) Aqueous Pollution by Reuse of Iron-Contaminated Water Treatment Residues

Marius Gheju and Ionel Balcu

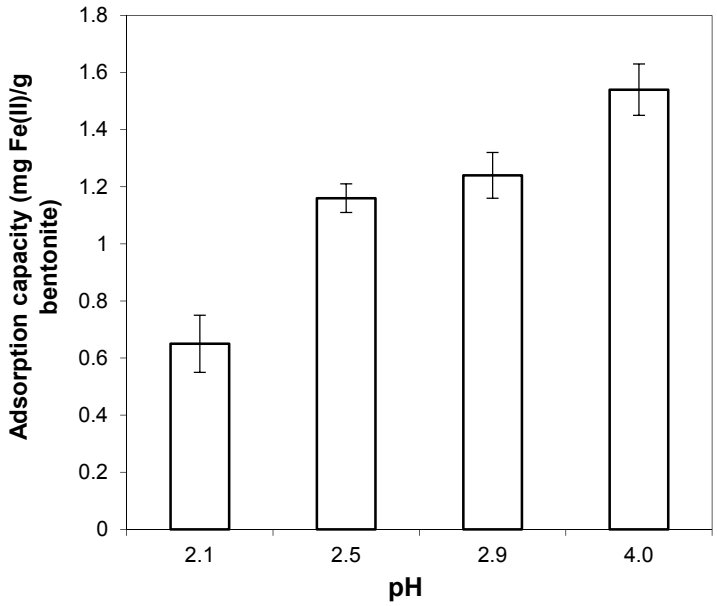

Figure S1. Effect of pH on bentonite Fe(II) adsorption capacity.

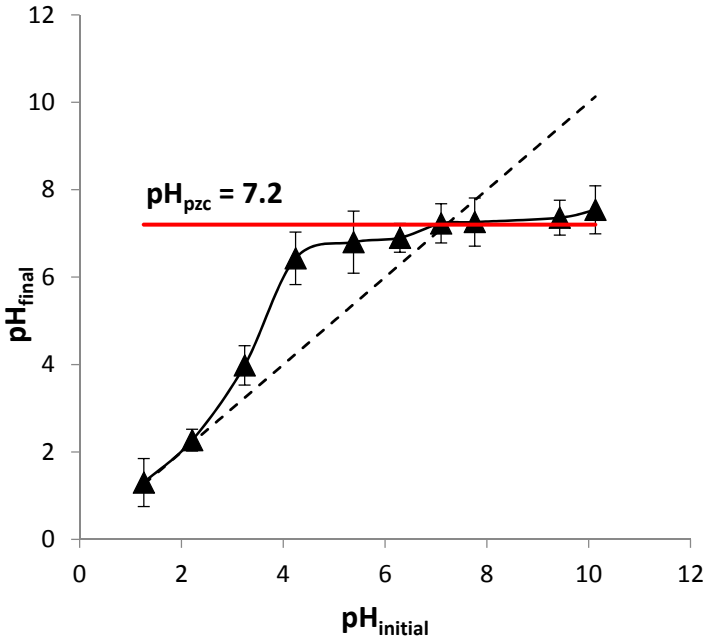

Figure S2. Plot of pH_{final} vs $pH_{initial}$ for the determination of bentonite pH_{pzc}.

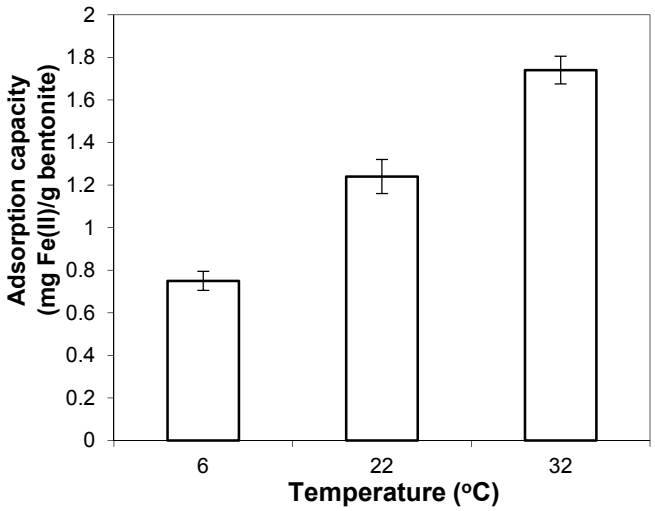

Figure S3. Effect of temperature on bentonite Fe(II) adsorption capacity.

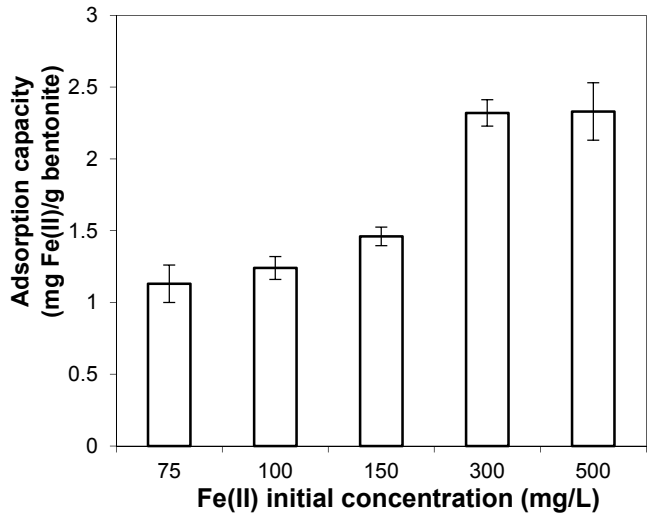

Figure S4. Effect of Fe(II) initial concentration on bentonite Fe(II) adsorption capacity.

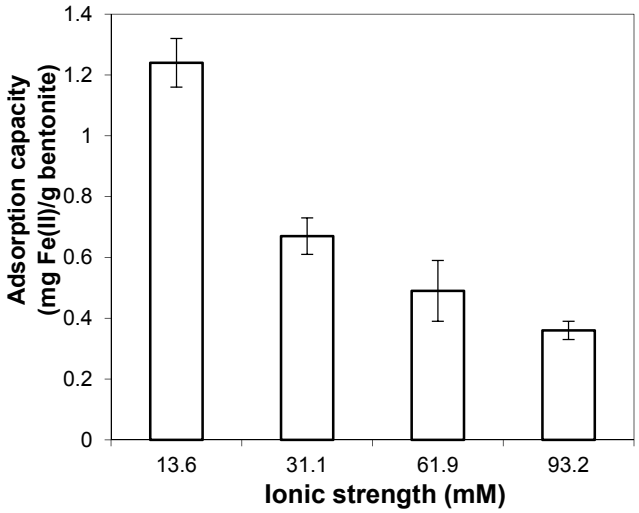

Figure S5. Effect of ionic strength on bentonite Fe(II) adsorption capacity.

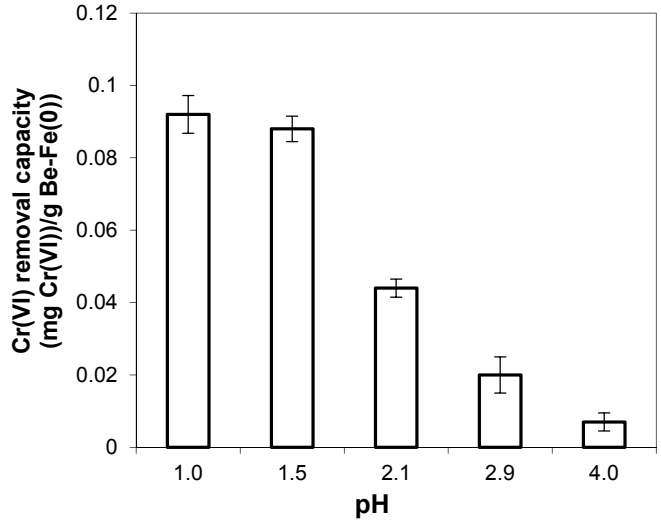

Figure S6. Effect of pH on Be-Fe(0) Cr(VI) removal capacity.

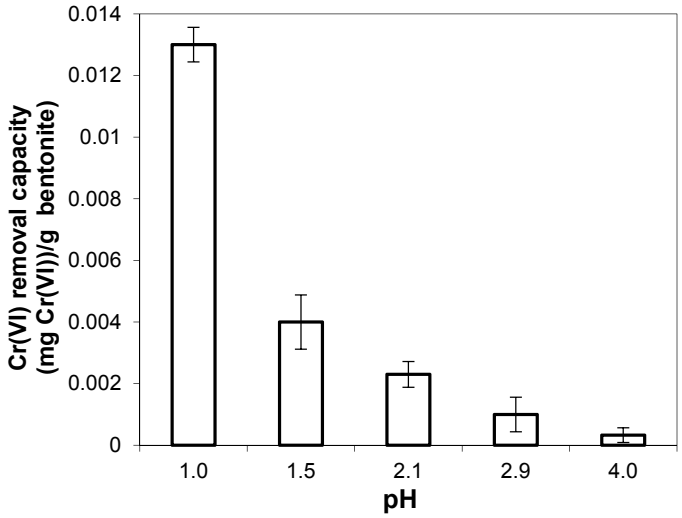

Figure S7. Effect of pH on bentonite Cr(VI) removal capacity.

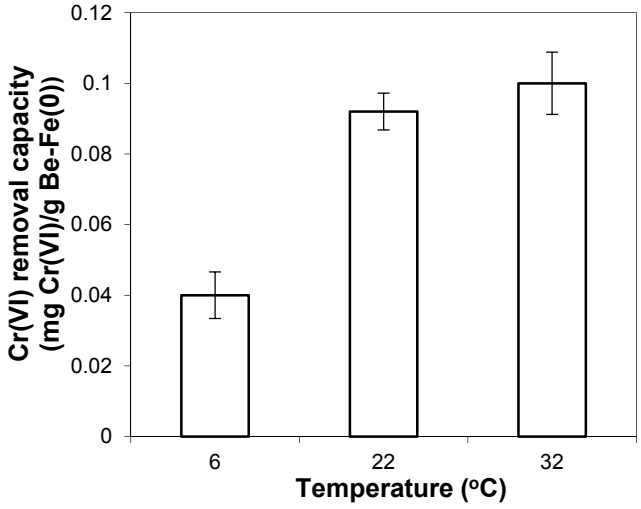

Figure S8. Effect of temperature on Be-Fe(0) Cr(VI) removal capacity.

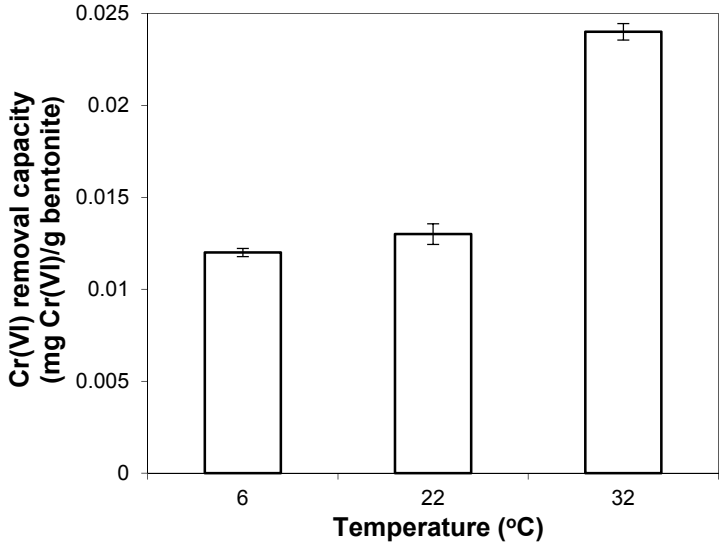

Figure S9. Effect of temperature on bentonite Cr(VI) removal capacity.

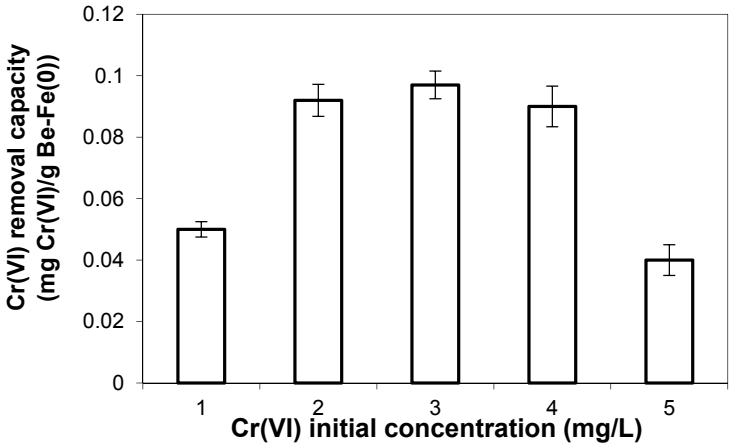

Figure S10. Effect of Cr(VI) initial concentration on Be-Fe(0) Cr(VI) removal capacity.

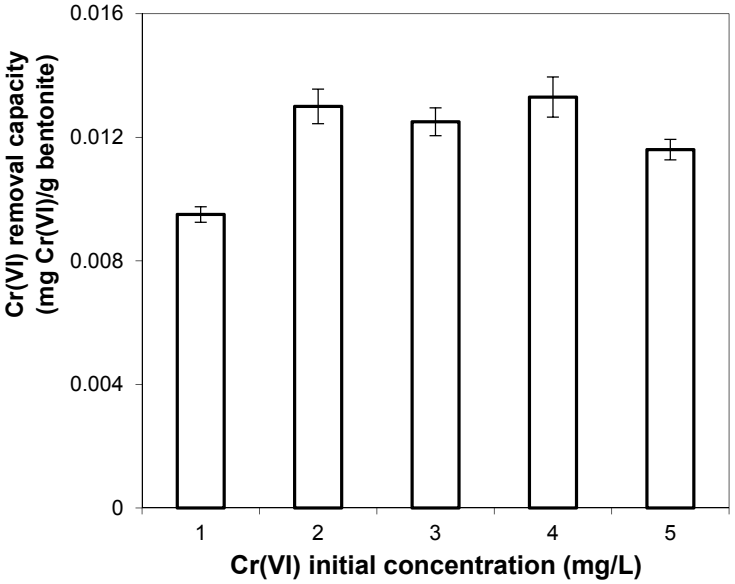

Figure S11. Effect of Cr(VI) initial concentration on bentonite Cr(VI) removal capacity.

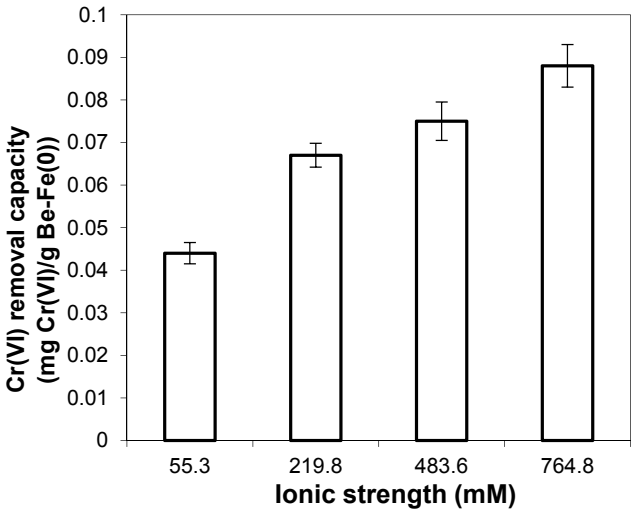

Figure S12. Effect of ionic strength on Be-Fe(0) Cr(VI) removal capacity.

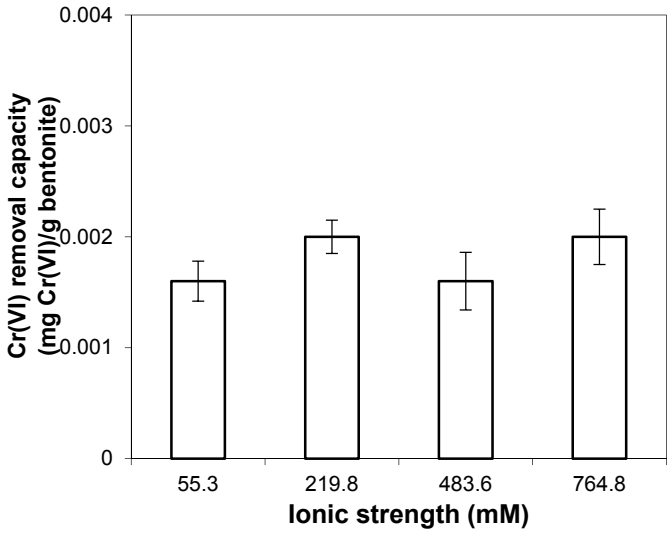

Figure S13. Effect of ionic strength on bentonite Cr(VI) removal capacity.

Figure S14. Image of fresh bentonite (A) and Be-Fe(0) (B).

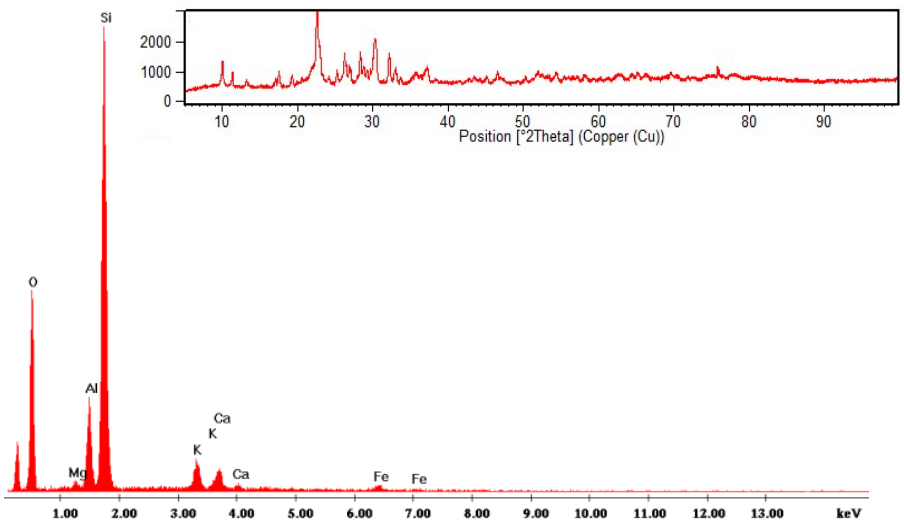

Figure S15. EDS and XRD pattern of fresh bentonite.

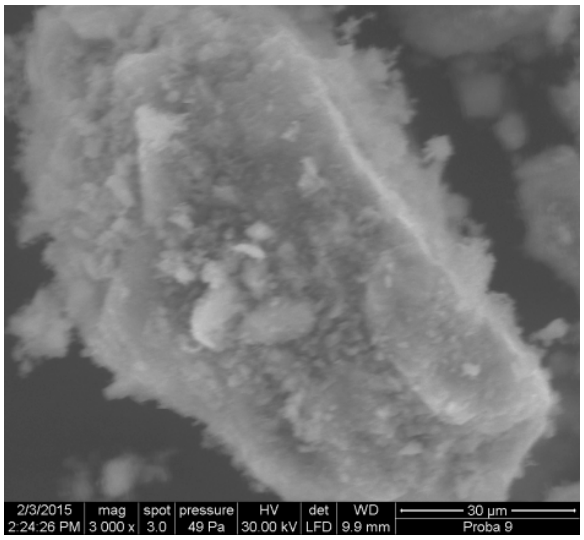

Figure S16. SEM micrograph of fresh bentonite.

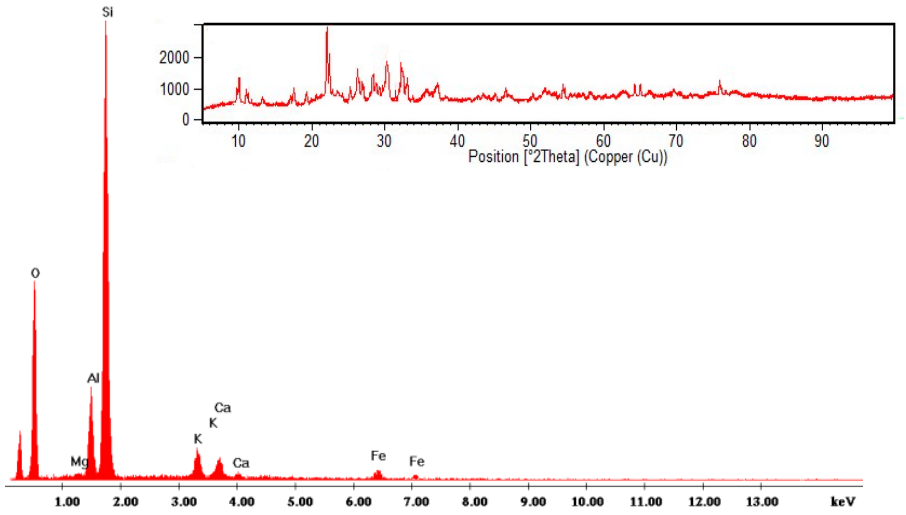

Figure S17. EDS and XRD pattern of exhausted bentonite after treatment of acid mine drainage.

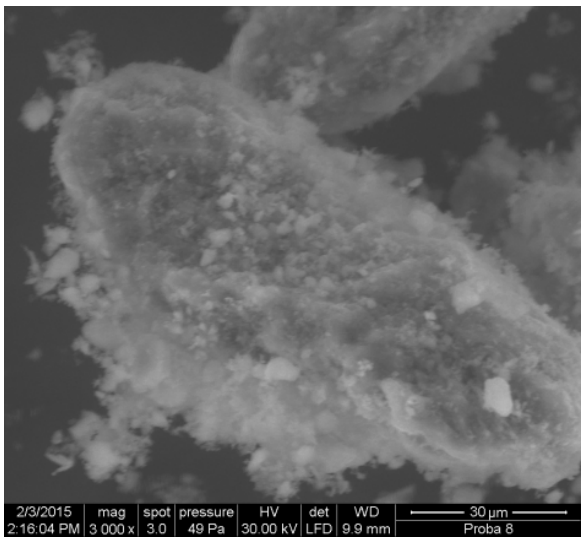

Figure S18. SEM micrograph of exhausted bentonite after treatment of acid mine drainage.

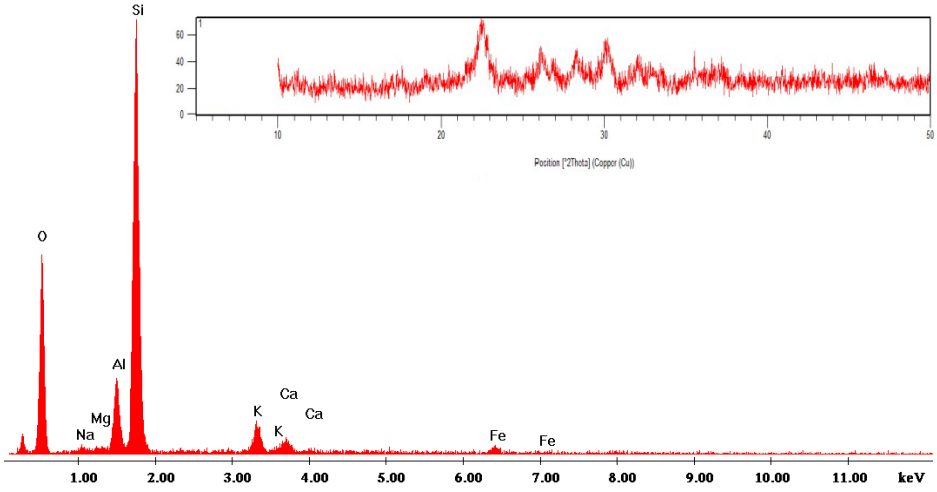

Figure S19. EDS and XRD pattern of fresh Be-Fe(0).

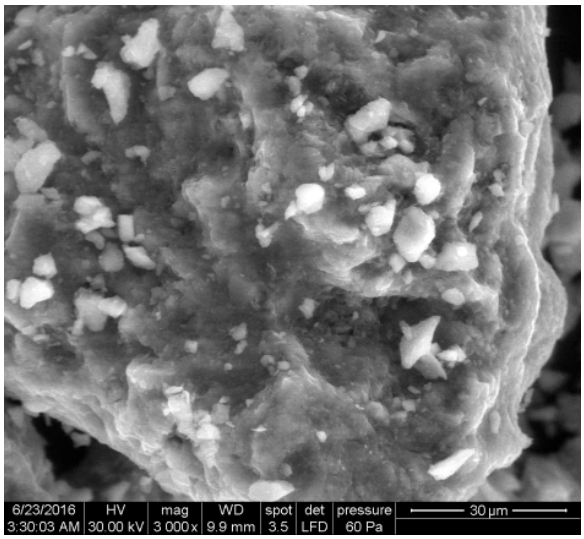

Figure S20. SEM micrograph of fresh Be-Fe(0).

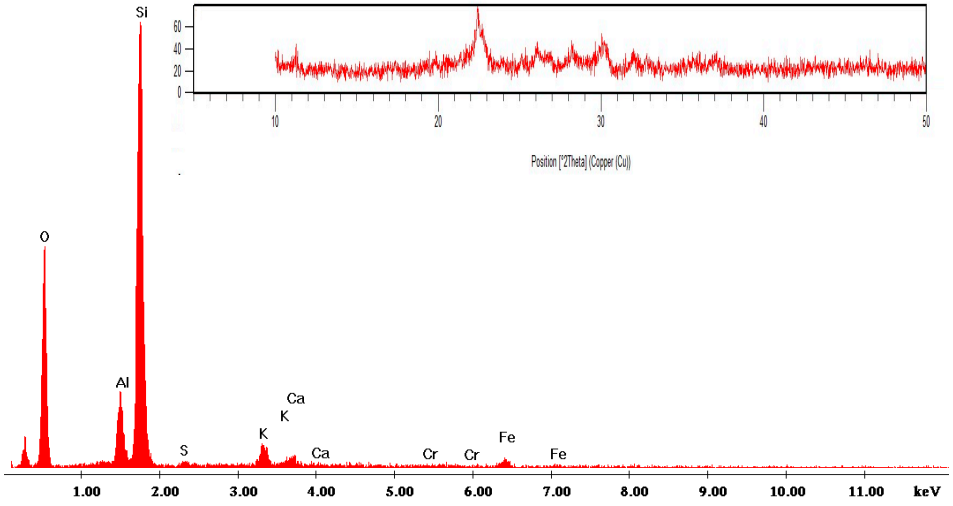

Figure S21. EDS and XRD pattern of exhausted Be-Fe(0) after treatment of Cr(VI) solution.

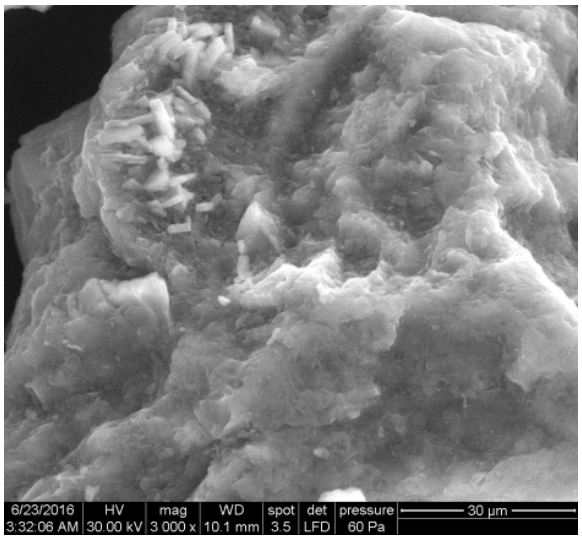

Figure S22. SEM micrograph of exhausted Be-Fe(0) after treatment of Cr(VI) solution.

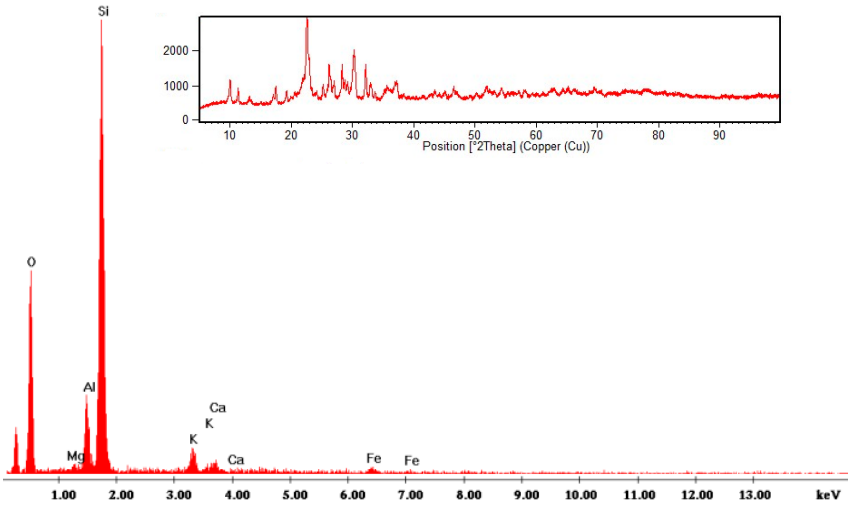

Figure S23. EDS and XRD pattern of exhausted bentonite after treatment of Cr(VI) solution.

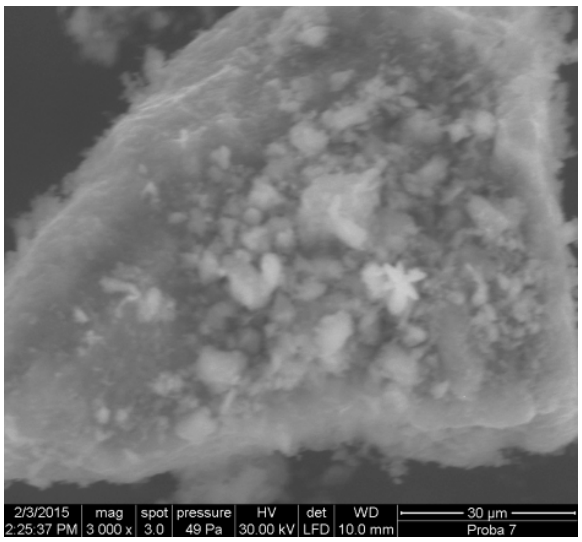

Figure S24. SEM micrograph of exhausted bentonite after treatment of Cr(VI) solution.

Calculation of Thermodynamic Parameters

The thermodynamic parameters Gibbs free energy of adsorption (ΔG), enthalpy change (ΔH), entropy change (ΔS) were computed by using data of Cr(VI) adsorption at temperatures of 6, 22 and 32 °C. The equilibrium constant K_c (L/g) of the Fe(II)/Cr(VI) process was evaluated using the following relationship:

$$K_c = \frac{C_{ads}^e}{C_{aq}^e} \quad \text{(S1)}$$

where C^e_{ads} is the equilibrium concentration of Cr(VI) on the adsorbent (mg g^{-1}) and C^e_{aq} is the equilibrium concentration of Cr(VI) in the aqueous solution (mg/L). Then, values of ΔG as a function of temperature were determined using van't Hoff equation:

$$\Delta G = -R \cdot T \cdot \ln K_c \quad \text{(S2)}$$

where K_c (L/mol) is the equilibrium constant, R (8.314 J mol^{-1} K^{-1}) is the universal gas constant and T (K) is the absolute temperature. Subsequently, ΔH and ΔS were computed from the slope and intercept of the Gibbs isotherm, by plotting ΔG versus T:

$$\Delta G = \Delta H - T \cdot \Delta S \quad \text{(S3)}$$

Table S1. Thermodynamic parameters of Fe(II) and Cr(VI) removal

Reactive system	Δ*G* (kJ/mol)			Δ*H*	Δ*S*
	T = 279.15 K	*T* = 295.15 K	*T* = 305.15 K	(kJ/mol)	(J/mol)
Bentonite + Fe(II)	0.52	−0.30	−1.87	26.06	91.0
Bentonite + Cr(VI)	1.30	0.37	−2.42	40.98	141.0
Be-Fe(0) + Cr(VI)	−1.27	−3.68	−32.31	328.52	1165.7